Dormancy within *Staphylococcus epidermidis* biofilms: a transcriptomic analysis by RNA-seq. **Applied Microbiology and Biotechnology** (2014) 98:2585–96

Virginia Carvalhais[a,b,c], Angela França[a,c], Filipe Cerca[d], Rui Vitorino[b], Gerald B Pier[c], Manuel Vilanova[d], Nuno Cerca[a*]

[a] IBB - Institute for Biotechnology and Bioengineering, Centre of Biological Engineering, University of Minho, Braga, Portugal
[b] QOPNA, Mass Spectrometry Center, Department of Chemistry, University of Aveiro, Portugal
[c] Division of Infectious diseases, Department of Medicine, Brigham and Women's Hospital, Harvard Medical School, Boston, Massachusetts, USA
[d] ICBAS – Instituto de Ciências Biomédicas de Abel Salazar, Universidade do Porto, Porto, Portugal
* Corresponding author: nunocerca@ceb.uminho.pt

Abstract
The proportion of dormant bacteria within *Staphylococcus epidermidis* biofilms may determine its inflammatory profile. Previously we have shown that *S. epidermidis* biofilms with higher proportions of dormant bacteria have reduced activation of murine macrophages. RNA-sequencing was used to identify the major transcriptomic differences between *S. epidermidis* biofilms with different proportions of dormant bacteria. To accomplish this goal, we used an in vitro model where magnesium allowed modulation of the proportion of dormant bacteria within *S. epidermidis* biofilms. Significant differences were found in the expression of 147 genes. A detailed analysis of the results was performed based on direct and functional gene interactions. Biological processes among the differentially expressed genes were mainly related to oxidation-reduction processes and acetyl-CoA metabolic processes. Gene-set enrichment revealed that the translation process is related to the proportion of dormant bacteria. Transcription of mRNAs involved in oxidation-reduction processes was associated with higher proportions of dormant bacteria within *S. epidermidis* biofilm. Moreover, pH of the culture medium did not change after the addition of magnesium and genes related to magnesium transport did not seem to impact entrance of bacterial cells into dormancy.

Introduction

Staphylococcus epidermidis is one of the major biofilm-producing bacteria which often colonize indwelling medical devices [1]. Establishment of biofilms is frequently associated with antimicrobial tolerance that can be explained, in part, by the presence of a sub-population of cells in a reversible non-replicative state which consequently can maintain a recalcitrant infection [2,3]. These cells can be defined as being in a dormant state, generally presenting a low-metabolism, allowing them to survive and resist under stressful conditions such as reduced availability of nutrients, oxygen starvation, temperature variation, salinity and pH variation [4,5]. Dormant cells may lead to misleading interpretations about the infection status of indwelling devices as they often do not grow on standard laboratory culture media [6]. Nevertheless, dormancy is a reversible state [7] and virulence properties of dormant bacteria may manifest as they transit into a growing state [8]. Dormancy improves long-term bacterial survival and facilitates pathogenesis [9] by increasing cellular tolerance to antibiotics [10-12] and evasion of the host immune system [13,14].

Persisters have been defined as "a small subpopulation of cells that spontaneously go into a dormant, non-dividing state" [15] and tolerate high concentrations of bactericidal agents [16]. Despite being dormant, further characteristics of persisters are still under debate [17,18]. Moreover, not all dormant bacteria are persisters [19,20]. In order to characterize dormant

persister bacteria, some approaches have been proposed and used to isolate these cells from *Escherichia coli* cultures (reviewed in [21]), namely by killing growing bacterial cells with antibiotics [22] or by separation of cells based on the lack of expression of degradable Green Fluorescent Protein [23]. In addition, we recently described how SYBR® green, a fluorochrome used to evaluate microbial viability via binding to nucleic acids, can be used to assess the metabolic state of *S. epidermidis* bacteria [24]. An in vitro model, using specific culture conditions, was used to modulate the proportions of dormant bacteria within *S. epidermidis* biofilms [25]. Accordingly to this model, the culture medium acidification, due to glucose metabolism, was responsible for inducing bacteria into a dormant state [13]. In contrast, this effect was found to be prevented by the addition of magnesium (Mg^{2+}) to the culture medium [25]. Magnesium action on *S. epidermidis* adhesion was previously shown by Dunne and Burd [26], however, the Mg^{2+} effect in biofilm maturation and its role on dormancy is still poorly understood [27,28].

The purpose of our study was to describe the major transcriptomic features of *S. epidermidis* biofilms, with induced or prevented dormancy, using high-throughput RNA-sequencing (RNA-seq). RNA-seq has been used for transcriptome analysis as an alternative to other transcriptomic technologies such as microarrays, due to advantages such as the large dynamic range, high technical reproducibility and a fact that a reference transcriptome is not a requirement [29-31]. RNA-seq has been applied to prokaryotic transcriptome studies [32,33] and some efforts have been made to use next-generation sequencing in clinical microbiology to test the properties of growing bacterial pathogens [34]. Global transcriptomic profile studies in *E. coli* and *Mycobacterium tuberculosis* dormant persister sub-population have been previously carried out, being reported the dormant state was associated with changes in transcription of genes involved in metabolism, biosynthetic pathways or oxidative stress [23,35].

To achieve our goal, we performed RNA-seq, of three biological triplicates, from the two distinct conditions previously described and we used a data analysis approach, based on direct and functional gene interactions, namely gene set-enrichment and cluster analysis.

Materials and Methods

Biofilm growth conditions

S. epidermidis strain 9142 (isolated from blood culture by [36] (collection number 18857 at DSM, Braunschweig, Germany) was used to establish biofilms with higher and lower ratios of dormant cells, as previously described [13]. Briefly, one colony of strain *S. epidermidis* 9142 was inoculated in Tryptic Soy Broth (TSB) (Becton, Dickinson and Company, Franklin Lakes, NJ, USA) and incubated at 37ºC in a shaker at 120 rpm for 18 hours. The overnight culture was adjusted to an optical density at 640 nm of 0.250 (±0.05) with TSB and 10 µL of this suspension was transferred into a 24-well plate (COSTAR, Corning Incorporated, Tewksbury, MA, USA) containing 1 mL of TSB supplemented with 0.4% glucose (v/v) (TSB 0.4% G) (American Bioanalytical, Natick, MA, USA) or TSB 0.4% G enriched with 20 mM magnesium chloride ($MgCl_2$) (American Bioanalytical). The culture plates were then incubated at 37ºC in a shaker at 120 rpm for 24 hours. After this period, the culture medium covering the biofilm was removed and replaced by fresh TSB supplemented with 1% glucose (v/v) (TSB 1% G) or TSB 1% G containing 20 mM $MgCl_2$ (TSB 1% G + Mg^{2+}). Biofilms were then allowed to grow in these same conditions for 24 additional hours. Next, biofilm culture medium was removed and biofilms were washed twice with 1× phosphate buffered saline (PBS) (Boston BioProducts, Boston, MA, USA). Then, bacteria within the biofilms were recovered in 1 mL of PBS. All tubes were placed on ice, to inhibit cell growth. Prior to preparation of the RNA-seq library, biofilm dormancy was assessed, as previously described [13]. Briefly, biofilms from both conditions were grown with the same initial amount of cells. Number of colony forming units (CFU/ mL) in each condition was determined using the spread plate method in Trypticase™ Soy Agar with 5% Sheep Blood (TSA II™) (Becton, Dickinson and Company).

RNA extraction

Total RNA was extracted using the RNeasy Mini kit (Qiagen, Valencia, CA, USA). To remove genomic DNA, Ambion® TURBO DNA-free™ kit (Invitrogen, Grand Island, NY, USA) was used followed by acid-phenol:chloroform precipitation (Ambion, Austin, Texas, USA), both following

the manufacturer's instructions. RNA integrity was determined using the Bioanalyzer 2100 (Agilent Technologies, Santa Clara, CA, USA), and samples with RNA Integrity Number (RIN) above 8 were selected for complementary DNA (cDNA) library preparation. Three independent biological experiments, each one from a pool of four biofilms, were performed.

cDNA library preparation and Sequencing

Before library preparation, ribosomal RNA (rRNA) was depleted from total RNA samples using the Ribo-Zero™ Magnetic kit for Gram-Positive bacteria (Epicentre, Madison, WI, USA), following the manufacturer's specifications. An Illumina® TruSeq™ RNA Sample Preparation kit (Illumina, San Diego, CA, USA) was used with the already purified mRNA, following the manufacturer's protocol. The construction of the libraries was rigorously validated by quantitative PCR and Hi-Sensitivity D1K TapeStation (Agilent 2200 TapeStation). Sequencing data were generated from paired-end reads (2 × 150bp) on a MiSeq® system (Illumina) using a RNA-seq library of 10 nM.

RNA sequencing data analyses

The removal of sequence adapters, mapping to reference genome and normalization of gene expression was performed using CLC Genomics Workbench software (V.5.5.1, CLC Bio.). RNA-seq reads were aligned to the reference genome of *S. epidermidis* strain RP62A (GenBank accession number NC_002976). Gene expression was normalized by calculating Reads per Kilobase per Million Mapped Reads (RPKM) using the methods described by Mortazavi and colleagues [37] in which normalization is adjusted by the counts of reads per kilobase per million mapped and gene length. Since consistency between experiments is a natural concern in RNA-seq, Pearson correlation was used to compare RPKM values between triplicates. To test for significant gene expression changes, Baggerley's test (beta-binominal) [38] with false discovery rate (FDR) correction was applied [39]. A *p*-value ≤0.05 was considered statistically significant. Venn diagram was generated using the Venny tool from BioinfoGP [40] to identify the transcripts uniquely expressed in each condition.

Biological interactions

Gene Ontology (GO) [41] and KEGG (Kyoto Encyclopedia of Genes and Genomes) pathways [42] analysis were performed to determine the function of differentially expressed genes, using STRING database (Search Tool for the Retrieval of Interacting Genes/Proteins) (version 9.05) [43]. Classes with a *p*-value ≤0.05 were considered statistically significant. Further analysis was carried out using Cytoscape software (version 2.8.3) [44], namely a gene-set enrichment analysis for over- and down-representation in the set of genes with a 1.50 fold-expression change and their neighbors [45], and a cluster analysis with MCODE plugin [46]. Biological interpretation was carried out using STRING bioinformatic tool.

Quantitative PCR

In order to validate the RNA-seq data, quantitative PCR (qPCR) was performed to quantify the mRNA transcripts of *pgi*, *gapA-2*, *acnA*, *ureA*, *ctsR* and *rplE.* The primers were designed with Primer3 software [47] and are shown in Supplementary Material (Table S2). 1 µg of total RNA was reverse transcribed using RevertAid First strand cDNA synthesis (ThermoScientific, Waltham, MA, USA) using random primers (NZYTech, Lisbon, Portugal). The experiment was performed using iQ SYBR 2× green supermix (Bio-Rad, Hercules, CA, USA) and CFX96™ thermocycler (Bio-Rad) with the following cycling parameters: 10 min at 95 °C followed by 40 repeats of 5 s at 95 °C, 10 s at 60 °C, and finally 20 s at 72 °C. The cycle threshold values (C_T) were determined and the relative fold differences were calculated by the $2^{(C_T \text{ reference gene} - C_T \text{ target gene})}$ method [48] using 16S rRNA as the reference gene. Three independent experiments were run in triplicate. Statistical significance was analyzed using unpaired t-test (with GraphPad Prism version 6, GraphPad Software Inc., La Jolla, CA, USA).

pH and Mg^{2+} measurements

To evaluate the culture pH and Mg^{2+} concentration in the culture medium over time, supernatant aliquots of *S. epidermidis* biofilms were collected every 3 hours during the last 24 hours of biofilm growth. Collected supernatants were centrifuged at 20.800 *g* for 5 min at 4 ºC and stored at -20 ºC before use. Culture pH was determined with a pH meter (WTW pH 330, Sigma-Aldrich

Inc., St. Louis, MO, USA). Mg^{2+} concentration was determined using atomic absorption spectrometry (Perkin-Elmer 5000, PerkinElmer,Inc., Waltham, MA, USA), according to the manufacturer's instructions. At least, two independent experiments were performed.

Results

Transcriptome analysis

We used RNA-seq technology to characterize the transcriptome of *S. epidermidis* biofilms with different proportions of dormant cells. Total RNA was isolated from three biologic replicates of cells within *S. epidermidis* biofilms grown in excess glucose with (prevented dormancy) or without Mg^{2+} (induced dormancy). As expected [13], the number of culturable bacteria in biofilms grown in TSB 1% G was lower than the number of CFU/ mL of biofilms grown in TSB 1% G + Mg^{2+}, as shown in the Supplementary Material (Fig. S1).

After depletion of rRNA, cDNA libraries were constructed using Illumina® TruSeq™ RNA Sample Preparation kit and MiSeq® sequencing system. An average of 3,029,921 (TSB 1% G) and 2,650,647 (TSB 1% G + Mg^{2+}) sequencing reads were obtained for each cDNA library. A global comparison of genes between biological triplicates showed a high correlation ($r>0.98$, Pearson's Correlation Coefficient for biofilms grown in TSB 1%G and $r\geq0.95$ for biofilms grown in TSB 1% G + Mg^{2+}). Before trimming the raw data, a Venn diagram was constructed (Fig. 1) to summarize the overlap between genes expressed in each condition.

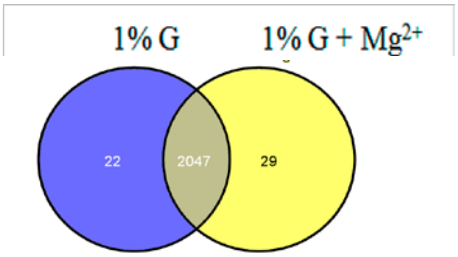

Fig. 1 | Venn diagram summarizing the overlap between genes with RPKM value above 1.00 in *S. epidermidis* biofilms grown in glucose excess with (1% G + Mg^{2+}) or without (1% G) magnesium

The expressed genes uniquely found in each condition with a RPKM above 1.00 encoded many uncharacterized proteins with unknown functions as shown in the Supplementary Material (Table S1). Nevertheless, among identified genes with higher RPKM values only found in *S. epidermidis* biofilms with induced dormancy was *mazE*, a gene which encodes an antitoxin component of a toxin-antitoxin module (*mazEF* module), and is related with the bacterial stress responses through mRNA degradation [49,50].

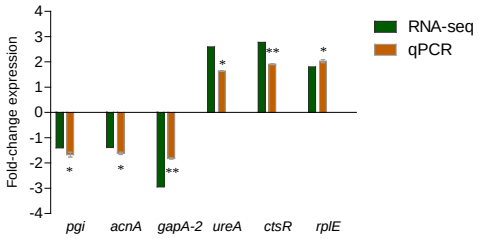

Fig. 2 qPCR validation of some differentially expressed genes. Fold-change expression is related to *S. epidermidis* biofilms grown in 1% G plus 20mM of Mg^{2+}. The bars represent the mean and the error bars the standard deviation. Statistical significance was analyzed using unpaired t-test (GraphPad Prism version 6). * $p<0.05$, ** $p<0.01$

For downstream applications, all genes with RPKM values under 1 were discarded. Thus, among the 2,047 genes identified as being transcribed in both conditions, 147 genes (7%) were differentially expressed between *S. epidermidis* biofilms with different proportions of dormant bacteria, wherein 28 (1%) were up-regulated and 119 (6%) were down-regulated. Additionally,

the distribution of the $\log_{10}$ RPKM among the differentially expressed genes of each biological triplicate also showed high agreement between the independent experiments, as in the Supplementary Material (Fig. S2). To further validate our data, qPCR was performed using a selection of up, or down-regulated genes, namely *pgi*, *acnA, gapA-2*, *ctsR*, *rplE* and *ureA* (Fig. 2).

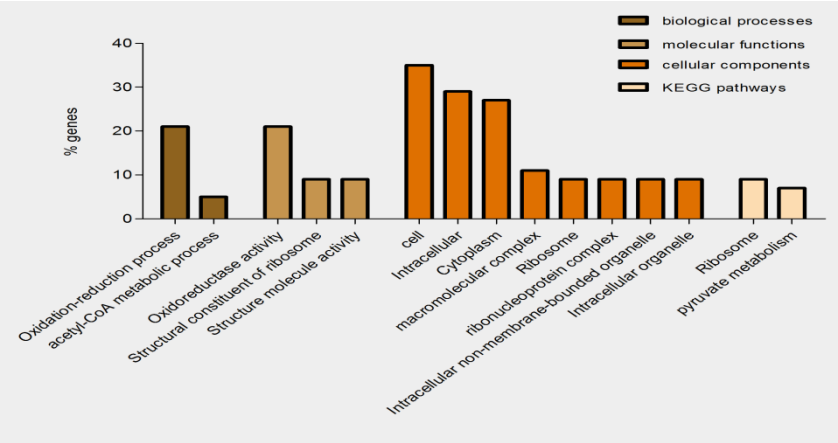

Fig. 3 Significant GO annotation and KEGG pathways of differentially expressed genes (p <0.05, FDR corrected). Biological processes (a), molecular functions (b), cellular components (c) and KEGG pathways (d)

Oxidation-reduction and acetyl-CoA metabolic processes were the significant biological processes found in the differently expressed genes. Oxido-reductase functions and ribosome activity were the significant molecular functions. Cytoplasm and intracellular components were the main cellular components represented in the differently expressed genes. The enriched KEGG pathways were for the ribosome synthesis pathway and pyruvate metabolism. In order to provide a more detailed analysis through pyruvate pathway, KEGG metabolic network was consulted and pyruvate cycle scheme was drawn to identify which enzymes involved in this pathway are encoded by the differentially expressed genes (Fig. 4).

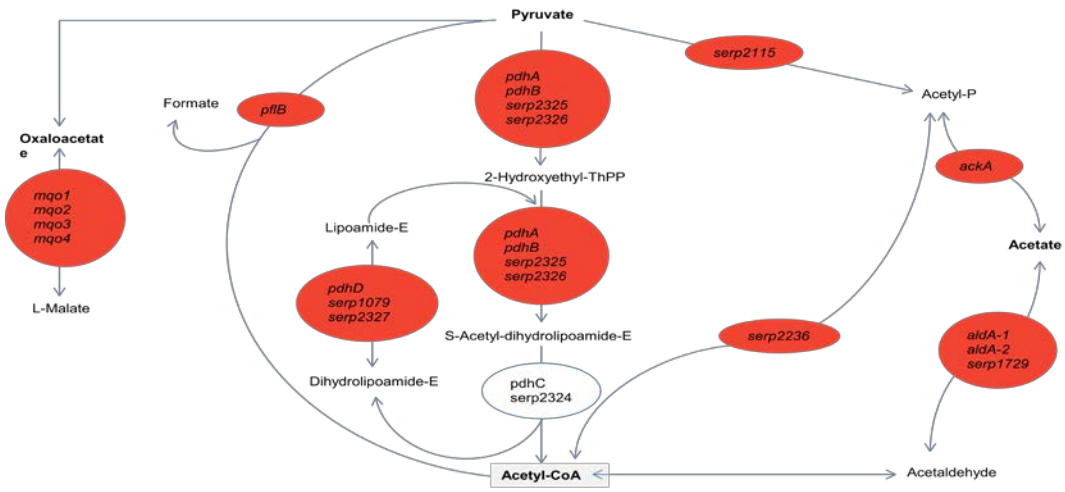

Fig. 4 Scheme of pyruvate metabolism and related products including genes which encode enzymes in each specific reaction. Red circles represent enzymes encoded by differentially expressed down-regulated genes in *S. epidermidis* biofilms grown in 1% G and Mg^{2+}.

Relevant biological processes and KEGG pathways within differentially expressed genes on replicates are shown in a heat map, constructed to depict fold-change values (Fig. 5). Gene expression analysis showed down-regulation of oxidation-reduction, pyruvate metabolism and acetyl-CoA metabolic processes in *S. epidermidis* biofilms with prevented dormancy, as

compared to biofilms with induced dormancy. Conversely, ribosome synthesis pathway was up-regulated in biofilms with dormancy prevented by Mg^{2+}. Twenty eight of the differentially expressed genes encoded uncharacterized proteins. In an attempt to find homology with known proteins, we performed a BLAST analysis, a search in the Pfam database (version 27.0) for Pfam domains [51] and PSORTb program (v. 3.0) [52] to predict their sub-cellular localization (Table 1).

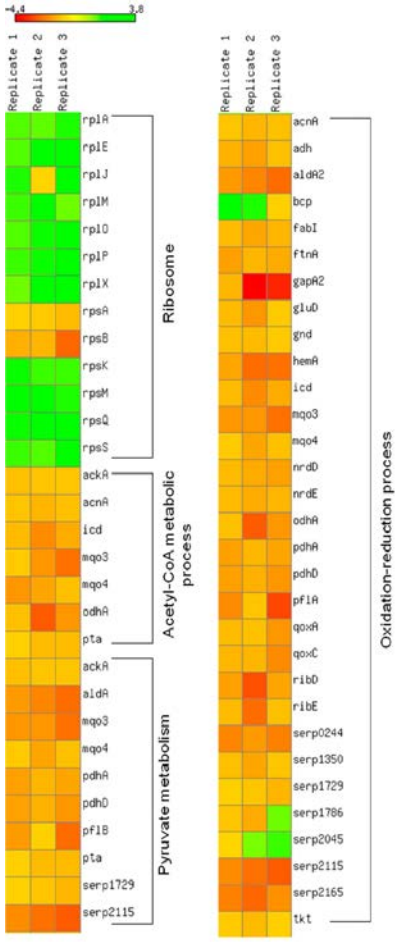

Fig. 5 Heat map of the main biological processes and KEGG pathways statistical significant in differentially expressed genes between induced and prevented dormancy of *S. epidermidis* biofilms. Values represent fold-change expression among biological triplicates. Red and green colors correspond to decrease and increase expression, respectively. Heat map was constructed using Matrix2png [75]

Although BLAST analysis indicated some homology with genes encoding uncharacterized proteins from other species (all these genes showed higher proximity to *Staphylococcus aureus Mu50*, except the *serp2066* gene which showed higher homology to *Macrococcus caseolyticus*), most of the predicted translated proteins would have a cytoplasm or cytoplasmic membrane localization. However, there were 15 proteins contained annotated domains in the Pfam database, indicating these were primarily domains with unknown functions.

Table 2 lists the 10 most highly and the 10 less transcribed genes based on RPKM values from *S. epidermidis* biofilms grown in TSB 1% G with Mg^{2+}. Although differences were not statistically significant, virulence genes seemed to be transcribed to a greater level in biofilms with induced dormancy.

Enrichment map analysis and cluster analysis

Downstream analysis of transcripts was based in direct and functional gene interactions using Cytoscape [54]. STRING was used to create a gene interaction network including all differentially expressed genes and neighbors, yielding a total of 1,442 nodes and 10,295 edges. GO analysis from the gene set-enrichment is given in Table 3.

Table 1. Differentially expressed genes representing uncharacterized proteins with significant Pfam domain, including predicted localization by PSORTb. ↑ means up-regulation and ↓ down-regulation in *S. epidermidis* biofilms grown in TSB 1% G enrich with Mg^{2+}.

Expression	Name	Function	Predicted localization	Protein family (Pfam) domain match
↑	*serp0087*	Uncharacterized protein	Cytoplasm	Uncharacterized conserved protein
↓	*serp0121*	Uncharacterized protein	Unknown	Protein of unknown function
↓	*serp0581*	UPF0413 protein	Cytoplasm	Thioredoxin
↓	*serp0701*	UPF0358 protein	Unknown	Protein of unknown function
↓	*serp0707*	Uncharacterized protein	Cytoplasmic membrane	Protein of unknown function
↑	*serp0741*	Uncharacterized N-acetyltransferase	Cytoplasm	Acetyltransferase (GNAT) domain
↓	*serp1053*	Uncharacterized protein	Cytoplasmic membrane	Protein of unknown function
↑	*serp1180*	Putative Holliday junction resolvase[a]	Unknown	Uncharacterized protein family
↓	*serp1210*	Uncharacterized protein	Cytoplasm	Protein of unknown function
↓	*serp1402*	Uncharacterized protein	Cytoplasmic membrane	Bacterial protein of unknown function
↓	*serp1720*	UPF0340 protein	Cytoplasm	Protein of unknown function
↓	*serp1754*	Uncharacterized protein	Cytoplasm	NADH(P)-binding
↓	*serp1771*	Uncharacterized protein	Cytoplasmic membrane	Domain of unknown function
↓	*serp1783*	Uncharacterized protein	Cytoplasmic membrane	Domain of unknown function
↑	*serp2066*	Uncharacterized protein	Cytoplasm	Domain of unknown function:

[a] Could be a nuclease that resolves Holliday junction intermediates in genetic recombination

Among the down-regulated and up-regulated transcripts in these *S. epidermidis* biofilms were genes mostly associated with oxidation-reduction and metabolic processes, respectively. Interestingly, most of the differentially expressed genes had a relatively small fold-change (-5.60 to 2.92), of which 13 of the up-regulated genes had a fold-change above 1.50 and 80 genes had a fold-change under -1.50. Fig. 6 shows RPKM values of a few *S. epidermidis* virulence genes, and genes related to biofilm formation, accumulation or modulation [1,53] among the two distinct conditions.

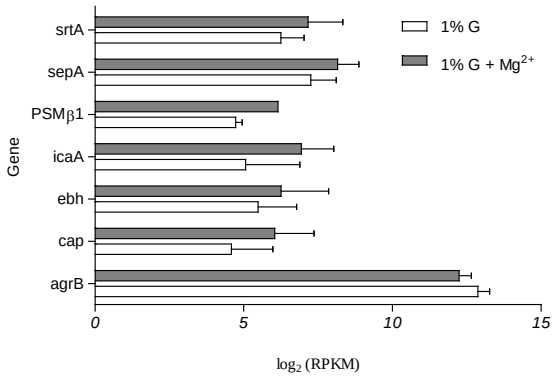

Fig. 6 Variation of $\log_2$(RPKM) among some known virulence genes in *S. epidermidis* biofilms grown with (1% G + Mg^{2+}) or without (1% G) magnesium. The bars represent the mean and the error bars the standard error of the mean.

Enrichment map analysis of the up-regulated and neighbor genes associated with *S. epidermidis* biofilms grown with Mg^{2+} revealed distinct functions involved in translation and biosynthetic processes, such as macromolecular synthesis. Conversely, down-regulated genes encoded catabolic processes and oxidoreductase activity. Gene clusters were obtained in Cytoscape with MCODE plugin. Among the differently expressed genes we found two clusters (a and b, in Fig. 7) with a score value above 2.0 and at least 4 nodes (complete gene network of differently expressed genes is shown in the Supplementary Material Fig. S3).

Table 2. List of the 10 genes with higher RPKM values among the differentially expressed genes, in *S. epidermidis* biofilms grown in TSB 1% G enrich with Mg^{2+}. Only genes with a fold-change expression ≤ -1.50 or ≥ 1.50 were included.

	Gene	Definition	RPKM 1% G	RPKM 1% G + Mg^{2+}	Fold-change	*p*-value (FDR corrected)
Rank down-regulated						
1	*serp1782*	Alkaline shock protein 23	18172.55	7034.27	-2.58	0.003
2	*serp0244*	Aldo/keto reductase	5885.19	2759.36	-2.13	<0.001
3	*pdhD*	Dihydrolipoamide dehydrogenase	4352.90	2433.65	-1.79	0.022
4	*pdhA*	Pyruvate dehydrogenase complex E1 component, alpha subunit	3908.68	2361.75	-1.65	0.026
5	*recA*[a]	Recombinase A	4788.63	1654.38	-2.89	<0.001
6	*serp1784*	Uncharacterized protein	4967.70	1624.00	-3.06	0.001
7	*mqo-4*	Malate:quinone oxidoreductase	3457.27	1590.09	-2.17	<0.001
8	*lexA*[a]	LexA repressor	3307.97	1571.21	-2.11	0.012
9	*aldA-2*	Aldehyde dehydrogenase	3645.71	1569.85	-2.32	0.011
10	*ptsI*	Phosphoenolpyruvate-protein phosphotransferase	2156.90	1350.52	-1.60	0.003
Rank up-regulated						
1	*serp0419*	Ribosomal subunit interface protein	4191.31	12241.98	2.92	0.018
2	*ctsR*	CtsR family transcriptional regulator	2279.57	6328.79	2.78	0.006
3	*serp0163*	UvrB/UvrC domain-containing protein	1885.05	4870.32	2.58	<0.001
4	*serp0164*	ATP:guanido phosphotransferase	1775.17	4289.27	2.42	0.031
5	*ppaC*	Manganese-dependent inorganic pyrophosphatase	443.67	861.75	1.94	<0.001
6	*rpsM*	30S ribosomal protein S13	425.78	698.09	1.64	<0.001
7	*serp1180*	Putative Holliday junction resolvase	368.63	583.88	1.58	<0.001
8	*rplE*	50S ribosomal protein L5	279.81	505.85	1.81	0.030
9	*ureA*	Urease subunit gamma	182.26	473.11	2.60	0.006
10	*rpsQ*	30S ribosomal protein S17	225.01	456.69	2.03	0.017

[a] LexA and RecA "changes the occurrence of persister cells in bacterial populations" [74]

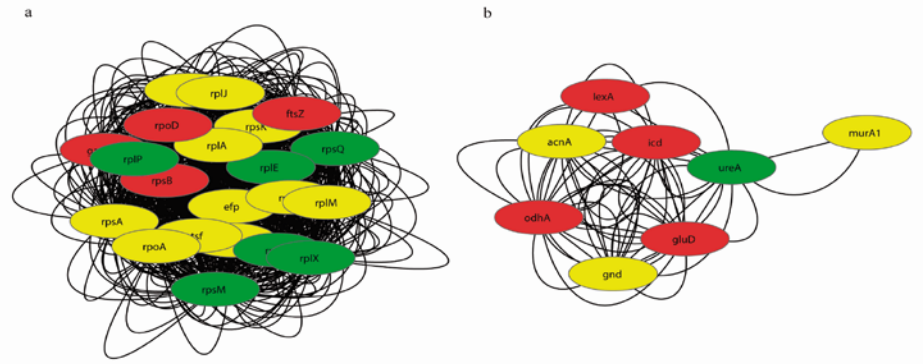

Fig. 7 Clusters generated by MCODE plug-in in Cytoscape, including fold-change expression. Red, green and yellow circles represent fold-change values under -1.50, above 1.50 and, between -1.50 and 1.50, respectively. Biological processes are translation and biosynthetic processes (a); and tricarboxylic acid cycle, acetyl-CoA catabolic process, coenzyme catabolic

process, cofactor catabolic process, acetyl-CoA metabolic process, aerobic respiration, cellular respiration, energy derivation by oxidation of organic compounds, coenzyme metabolic processes (b)

Table 3. Statistically significant biological processes from gene set-enrichment analysis.

Gene-set enrichment	Biological process	*p*-value (Bonferroni correction)
Up-regulation		
GO:0006412	Translation	4.56E-15
GO:0044267	Cellular protein metabolic process	2.52E-10
GO:0010467	Gene expression	3.75E-09
GO:0034645	Cellular macromolecule biosynthetic process	4.68E-09
GO:0019538	Protein metabolic process	8.31E-09
GO:0009059	Macromolecule biosynthetic process	8.58E-09
GO:0044249	Cellular biosynthetic process	2.89E-05
GO:0015986	ATP synthesis coupled proton transport	7.83E-05
GO:0009058	Biosynthetic process	1.84E-04
GO:0006754	ATP biosynthetic process	5.53E-04
GO:0044260	Cellular macromolecule metabolic process	1.07E-03
GO:0043170	Macromolecule metabolic process	4.97E-03
GO:0009142	Nucleoside triphosphate biosynthetic process	1.14E-02
GO:0034220	Ion transmembrane transport	1.14E-02
GO:0015992	Proton transport	2.65E-02
Down-regulation		
GO:0008152	Metabolic process	9.76E-04
GO:0055114	Oxidation-reduction process	1.44E-03
GO:0006006	Glucose metabolic process	2.16E-02

The main biological processes of each cluster were translation and biosynthetic processes (cluster a), and catabolic and oxidation-reduction processes (cluster b), which is in accordance with the results obtained in the gene set-enrichment.

Evaluation of culture medium pH and Mg^{2+} levels

Since acidic pH conditions have been described as an inhibitor of bacterial growth [55], we assessed whether the culture medium pH was altered and might be related to bacterial dormancy and consequently to transcriptomic differences observed when Mg^{2+} was added. We found that *S. epidermidis* biofilms grown in TSB 1% G enriched with $MgCl_2$ did not have an altered pH in the final culture medium as shown in Supplementary Material Fig. S4a. Furthermore, assessment of Mg^{2+} consumption over time showed that Mg^{2+} levels were constant, revealing that Mg^{2+} was not depleted from the culture medium in established biofilms, as shown in Supplementary Material Fig. S4b. These results indicate that, similar to the culture medium pH, the Mg^{2+} levels are maintained throughout the culture.

Discussion

It has been reported that cells in the deeper layers of the biofilms are less active than the ones in the upper layers, although they are still viable but with a slower growth and a lower metabolic rate [10]. Bacterial phenotypes can change according to environmental conditions and chemical-concentration gradients, generating distinct populations and contributing to heterogeneity within biofilms [56]. Dormancy can be considered an adaptive response to adverse environmental conditions. Since the survival capacity of dormant bacteria in biofilm-related infections is increased [11], it is of utmost importance to characterize *S. epidermidis* biofilms dormant sub-population. In order to improve mRNA quantitation by RNA-seq technology, many transcriptomic studies have tried to increase the information content by depleting rRNA [57]. Previous bacterial RNA-seq studies suggest that a minimum of 2–5 million reads from an rRNA-depleted library are required for accurate coverage (reviewed in [57]). Moreover, paired-end sequencing is a more efficient strategy to characterize and quantify the transcriptome of bacteria without annotated genomes [58]. Besides biological variability, technical issues like coverage [33], sequence depth [59], variation from one flow cell to another

[58], variation between the individual lanes within a flow cell [58] and library preparation effect [60] may also affect sequencing and cause variability within replicates. In order to overcome these limitations and to obtain more accurate results, we ran 3 biological replicates consisting of pools of 4 biofilms for each replicate. This approach contributed to the observed consistency in our data.

GO analysis has been used in genome-wide expression studies to reduce complexity and highlight biological processes [61]. GO analysis of the 147 differentially expressed genes between the two studied conditions identified ribosome activity, oxidation-reduction and acetyl-CoA metabolic processes as the major classes with differences in mRNA transcripts. The main biological processes and KEGG pathways showed consistency within gene expression levels among biological triplicates and evidence that genes involved in oxidation-reduction, acetyl-CoA metabolic processes and pyruvate metabolism were less expressed in biofilms with prevented dormancy. In the opposite, ribosome pathway was more expressed in *S. epidermidis* biofilms grown with Mg^{2+}. Differentially expressed genes encoded transcripts mostly localized in the intracellular compartments, suggesting that the major changes related to the development of dormancy are occurring within the cell cytoplasm. These results were expected since *S. epidermidis* biofilms grown in excess glucose and Mg^{2+} have a lower number of dormant bacteria and, consequently, more metabolically active cells. In addition, half of the most down-regulated gene transcripts in *S. epidermidis* biofilms grown with Mg^{2+} are involved in oxido-reductase activity, such as *serp0244*, *pdhA*, *pdhD*, *aldA* and *mqo3* (Table 2). Conversely, the most up-regulated genes are mainly related to metabolic processes. Previously, our group showed the impact on virulence of dormant *S. epidermidis* biofilm [13]. In the present work, biofilms with lower levels of dormant cells had an increased, but not significant, expression of some of the main virulence genes.

Glucose has a key role in biofilm physiology [14,36]. The major pathways for glucose catabolism in Staphylococci are glycolysis, the pentose-phosphate pathways and the tricarboxcylic acid cycle [62]. Allison et al. [63] showed that metabolites from the upper glycolysis pathway and pyruvate, in combination with aminoglycosides, may be used to treat biofilms with higher levels of dormant, persister cells, proposing a metabolic-based strategy to eradicate bacterial persisters. Not surprisingly, glucose has influence in biofilm physiology since glucose metabolism leads to accumulation of acidic products decreasing the pH of the culture medium [64]. The model that we previously described showed that dormancy was a consequence of excess of glucose catabolism that lead to the acidification of the culture medium and consequently to the accumulation of dormant bacteria within *S. epidermidis* biofilms [13]. This phenomenon was prevented by the presence of high extracellular levels of magnesium which did not change the pH of the culture medium, indicating that the Mg^{2+} effect on preventing cell dormancy was not related to the pH of the culture, since low pH was still maintained in the presence of Mg^{2+}. Low pH was previously associated with a loss of activity of glycolytic enzymes and damage to cell membrane and macromolecules such as proteins and DNA, and was related to changes in biogenesis and maintenance of cell membrane integrity (revised in [65]).

Piddington and colleagues demonstrated that Mg^{2+} is essential to *M. tuberculosis* growth in acidic conditions and it could not be replaced by other divalent cations [28]. A possible influence of Mg^{2+} in protein structure and physical properties was also described in *M. tuberculosis* [66]. Since the Mg^{2+} levels in biofilm cultures were maintained over time, similar to the pH in the culture medium, we performed a search of *S. epidermidis* enzymes whose co-factor was magnesium (in http://enzyme.expasy.org). Interestingly, among 20 enzyme-encoding genes, only 3 of these were encoded by genes found to be differentially expressed between the two distinct biofilm conditions, with a lower expression in biofilms grown with $MgCl_2$, suggesting that Mg^{2+} is not increasing the expression of genes encoding proteins using Mg^{2+} as a co-factor. In addition, genes related to the Mg^{2+} transport system, such as *corA*, *mgtE* and *serp1967* [67] were not differentially expressed, indicating that high Mg^{2+} levels culture are also not stimulating expression of magnesium transport genes.

Previous work with dormant bacterial cultures demonstrated decreased levels of macromolecule synthesis, nutrient transport and respiration rates (reviewed by [68]). Moreover, earlier transcriptomic studies of dormant persister cells of several microorganisms showed a down-regulation of energy and metabolism pathways [35], increased reactive oxygen species levels [69] and down-regulation of genes involved in energy production [23]. Toxin over-expression from toxin-antitoxin modules has been linked to the persister fraction in *E. coli* and *M. tuberculosis* cultures (reviewed in [70]). The toxin-antitoxin module *mazEF* is highly conserved in *Staphylococcus* species and was described in detail in *S. aureus*, where antitoxin MazE binds toxin MazF to neutralize ribonucleases activity [71], and more recently in *Staphylococcus equorum* [72]. Despite no alterations in *mazF* expression between S. *epidermidis* biofilms grown in the absence or presence of Mg^{2+}, *mazE* gene RPKM was superior to 1.00 in biofilms grown without Mg^{2+}.

Taken together, these results reveal that the transcription of genes involved in oxidation-reduction processes as well as glucose metabolism, was more active in dormant *S. epidermidis* biofilms, despite no differences in glucose consumption, probably due to lower metabolism of dormant bacteria. On the other hand, genes related to ribosome activity were up-regulated in *S. epidermidis* biofilms when Mg^{2+} levels were higher in the growth medium. Additionally, these results provide evidence that the genes directly involved in Mg^{2+} transport do not seem to have a direct role in the shift to dormancy. However, the global changes found in this work do not provide information only confined to the dormant bacterial cells. Most probably, differences among readily culturable and dormant bacterial cells are greater than those referenced here. Single-cell analysis methods are being developed and may allow a more accurate comparison between these physiological states [73]. Yet, dormant bacterial cell isolation is still a meaningful challenge.

Overall, these results contribute to a better understanding of the mechanisms underlying the dormancy phenomena. Nevertheless, these findings also raise questions regarding the role of dormant *S. epidermidis* biofilms in virulence, since it is still debatable if there is a lower virulence potential due to lower metabolism, or if expression of a specific gene or a set of genes could lead to the suppression of the host immune response.

Acknowledgements
The authors thank Stephen Lorry at Harvard Medical School for providing CLC Genomics software. This work was funded by Fundação para a Ciência e a Tecnologia (FCT) and COMPETE grants PTDC/BIA-MIC/113450/2009, FCOMP-01-0124-FEDER-014309, QOPNA research unit (project PEst-C/QUI/UI0062/2011) and CENTRO-07-ST24-FEDER-002034. The following authors had an individual FCT fellowship: VC (SFRH/BD/78235/2011); AF (SFRH/BD/62359/2009).

Reference List

[1] Otto M. Molecular basis of *Staphylococcus epidermidis* infections. Semin Immunopathol 2012 Mar;34(2):201-14.
[2] Fauvart M, De Groote VN, Michiels J. Role of persister cells in chronic infections: clinical relevance and perspectives on anti-persister therapies. J Med Microbiol 2011 Jun;60(Pt 6):699-709.
[3] Lewis K. Persister cells, dormancy and infectious disease. Nat Rev Microbiol 2007 Jan;5(1):48-56.
[4] Trevors JT. Viable but non-culturable (VBNC) bacteria: Gene expression in planktonic and biofilm cells. J Microbiol Methods 2011 Aug;86(2):266-73.
[5] Colwell RR. Viable but nonculturable bacteria: a survival strategy. J Infect Chemother 2000 Jun;6(2):121-5.
[6] Zandri G, Pasquaroli S, Vignaroli C, Talevi S, Manso E, Donelli G, et al. Detection of viable but non-culturable staphylococci in biofilms from central venous catheters negative on standard microbiological assays. Clin Microbiol Infect 2012 Jul;18(7):E259-E261.
[7] Kaprelyants AS, Gottschal JC, Kell DB. Dormancy in non-sporulating bacteria. FEMS Microbiol Rev 1993 Apr;10(3-4):271-85.
[8] Sun F, Chen J, Zhong L, Zhang XH, Wang R, Guo Q, et al. Characterization and virulence retention of viable but nonculturable Vibrio harveyi. FEMS Microbiol Ecol 2008 Apr;64(1):37-44.

[9] Dworkin J, Shah IM. Exit from dormancy in microbial organisms. Nat Rev Microbiol 2010 Dec;8(12):890-6.

[10] Williamson KS, Richards LA, Perez-Osorio AC, Pitts B, McInnerney K, Stewart PS, et al. Heterogeneity in *Pseudomonas aeruginosa* biofilms includes expression of ribosome hibernation factors in the antibiotic-tolerant subpopulation and hypoxia-induced stress response in the metabolically active population. J Bacteriol 2012 Apr;194(8):2062-73.

[11] Kim J, Hahn JS, Franklin MJ, Stewart PS, Yoon J. Tolerance of dormant and active cells in *Pseudomonas aeruginosa* PA01 biofilm to antimicrobial agents. J Antimicrob Chemother 2009 Jan;63(1):129-35.

[12] Shapiro JA, Nguyen VL, Chamberlain NR. Evidence for persisters in *Staphylococcus epidermidis* RP62a planktonic cultures and biofilms. J Med Microbiol 2011 Jul;60(Pt 7):950-60.

[13] Cerca F, Andrade F, Franca A, Andrade EB, Ribeiro A, Almeida AA, et al. *Staphylococcus epidermidis* biofilms with higher proportions of dormant bacteria induce a lower activation of murine macrophages. J Med Microbiol 2011 Dec;60(Pt 12):1717-24.

[14] Yao Y, Sturdevant DE, Otto M. Genomewide analysis of gene expression in *Staphylococcus epidermidis* biofilms: insights into the pathophysiology of *S. epidermidis* biofilms and the role of phenol-soluble modulins in formation of biofilms. J Infect Dis 2005 Jan 15;191(2):289-98.

[15] Lewis K. Persister cells: molecular mechanisms related to antibiotic tolerance. Handb Exp Pharmacol 2012;(211):121-33.

[16] Keren I, Kaldalu N, Spoering A, Wang Y, Lewis K. Persister cells and tolerance to antimicrobials. FEMS Microbiol Lett 2004 Jan 15;230(1):13-8.

[17] Allison KR, Brynildsen MP, Collins JJ. Heterogeneous bacterial persisters and engineering approaches to eliminate them. Curr Opin Microbiol 2011 Oct;14(5):593-8.

[18] Balaban NQ, Gerdes K, Lewis K, McKinney JD. A problem of persistence: still more questions than answers? Nat Rev Microbiol 2013 Aug;11(8):587-91.

[19] Jayaraman R. Bacterial persistence: some new insights into an old phenomenon. J Biosci 2008 Dec;33(5):795-805.

[20] Orman MA, Brynildsen MP. Dormancy is not necessary or sufficient for bacterial persistence. Antimicrob Agents Chemother 2013 Jul;57(7):3230-9.

[21] Lewis K. Persister cells. Annu Rev Microbiol 2010;64:357-72.

[22] Keren I, Shah D, Spoering A, Kaldalu N, Lewis K. Specialized persister cells and the mechanism of multidrug tolerance in *Escherichia coli*. J Bacteriol 2004 Dec;186(24):8172-80.

[23] Shah D, Zhang Z, Khodursky A, Kaldalu N, Kurg K, Lewis K. Persisters: a distinct physiological state of *E. coli*. BMC Microbiol 2006;6:53.

[24] Cerca F, Trigo G, Correia A, Cerca N, Azeredo J, Vilanova M. SYBR green as a fluorescent probe to evaluate the biofilm physiological state of *Staphylococcus epidermidis,* using flow cytometry. Can J Microbiol 2011 Oct;57(10):850-6.

[25] Cerca F, Franca A, Guimaraes R, Hinzmann M, Cerca N, Lobo dC, et al. Modulation of poly-N-acetylglucosamine accumulation within mature *Staphylococcus epidermidis* biofilms grown in excess glucose. Microbiol Immunol 2011 Oct;55(10):673-82.

[26] Dunne WMJr, Burd EM. The effects of magnesium, calcium, EDTA, and pH on the in vitro adhesion of *Staphylococcus epidermidis* to plastic. Microbiol Immunol 1992;36(10):1019-27.

[27] Song B, Leff LG. Influence of magnesium ions on biofilm formation by *Pseudomonas fluorescens*. Microbiol Res 2006;161(4):355-61.

[28] Piddington DL, Kashkouli A, Buchmeier NA. Growth of *Mycobacterium tuberculosis* in a defined medium is very restricted by acid pH and Mg(2+) levels. Infect Immun 2000 Aug;68(8):4518-22.

[29] Wang Z, Gerstein M, Snyder M. RNA-Seq: a revolutionary tool for transcriptomics. Nat Rev Genet 2009 Jan;10(1):57-63.

[30] Raz T, Kapranov P, Lipson D, Letovsky S, Milos PM, Thompson JF. Protocol dependence of sequencing-based gene expression measurements. PLoS One 2011;6(5):e19287.

[31] van Vliet AH. Next generation sequencing of microbial transcriptomes: challenges and opportunities. FEMS Microbiol Lett 2010 Jan;302(1):1-7.

[32] Sorek R, Cossart P. Prokaryotic transcriptomics: a new view on regulation, physiology and pathogenicity. Nat Rev Genet 2010 Jan;11(1):9-16.

[33] Croucher NJ, Thomson NR. Studying bacterial transcriptomes using RNA-seq. Curr Opin Microbiol 2010 Oct;13(5):619-24.

[34] Didelot X, Bowden R, Wilson DJ, Peto TE, Crook DW. Transforming clinical microbiology with bacterial genome sequencing. Nat Rev Genet 2012 Sep;13(9):601-12.

[35] Keren I, Minami S, Rubin E, Lewis K. Characterization and transcriptome analysis of *Mycobacterium tuberculosis* persisters. MBio 2011;2(3):e00100-e00111.

[36] Mack D, Siemssen N, Laufs R. Parallel induction by glucose of ahderence and a polysaccharide antigen specific for plastic-adherent *Staphylococcus epidermidis*: evidence for functional relation to intercellular adhesion. Infect Immun 1992;60:2048-57.

[37] Mortazavi A, Williams BA, McCue K, Schaeffer L, Wold B. Mapping and quantifying mammalian transcriptomes by RNA-Seq. Nat Methods 2008 Jul;5(7):621-8.

[38] Baggerly KA, Deng L, Morris JS, Aldaz CM. Differential expression in SAGE: accounting for normal between-library variation. Bioinformatics 2003 Aug 12;19(12):1477-83.
[39] Pawitan Y, Michiels S, Koscielny S, Gusnanto A, Ploner A. False discovery rate, sensitivity and sample size for microarray studies. Bioinformatics 2005 Jul 1;21(13):3017-24.
[40] Oliveros JC. VENNY. An interactive tool for comparing lists with Venn Diagrams. http://bioinfogp cnb csic es/tools/venny/ 2007
[41] Ashburner M, Ball CA, Blake JA, Botstein D, Butler H, Cherry JM, et al. Gene ontology: tool for the unification of biology. The Gene Ontology Consortium. Nat Genet 2000 May;25(1):25-9.
[42] Kanehisa M, Goto S, Kawashima S, Okuno Y, Hattori M. The KEGG resource for deciphering the genome. Nucleic Acids Res 2004 Jan 1;32(Database issue):D277-D280.
[43] Franceschini A, Szklarczyk D, Frankild S, Kuhn M, Simonovic M, Roth A, et al. STRING v9.1: protein-protein interaction networks, with increased coverage and integration. Nucleic Acids Res 2013 Jan;41(Database issue):D808-D815.
[44] Shannon P, Markiel A, Ozier O, Baliga NS, Wang JT, Ramage D, et al. Cytoscape: a software environment for integrated models of biomolecular interaction networks. Genome Res 2003 Nov;13(11):2498-504.
[45] Merico D, Isserlin R, Stueker O, Emili A, Bader GD. Enrichment map: a network-based method for gene-set enrichment visualization and interpretation. PLoS One 2010;5(11):e13984.
[46] Bader GD, Hogue CW. An automated method for finding molecular complexes in large protein interaction networks. BMC Bioinformatics 2003 Jan 13;4:2.
[47] Rozen S, Skaletsky H. Primer3 on the WWW for general users and for biologist programmers. Methods Mol Biol 2000;132:365-86.
[48] Livak KJ, Schmittgen TD. Analysis of relative gene expression data using real-time quantitative PCR and the 2(-Delta Delta C(T)) Method. Methods 2001 Dec;25(4):402-8.
[49] Zorzini V, Haesaerts S, Donegan NP, Fu Z, Cheung AL, van Nuland NA, et al. Crystallization of the *Staphylococcus aureus* MazF mRNA interferase. Acta Crystallogr Sect F Struct Biol Cryst Commun 2011 Mar 1;67(Pt 3):386-9.
[50] Mittenhuber G. Occurrence of mazEF-like antitoxin/toxin systems in bacteria. J Mol Microbiol Biotechnol 1999 Nov;1(2):295-302.
[51] Punta M, Coggill PC, Eberhardt RY, Mistry J, Tate J, Boursnell C, et al. The Pfam protein families database. Nucleic Acids Res 2012 Jan;40(Database issue):D290-D301.
[52] Yu NY, Wagner JR, Laird MR, Melli G, Rey S, Lo R, et al. PSORTb 3.0: improved protein subcellular localization prediction with refined localization subcategories and predictive capabilities for all prokaryotes. Bioinformatics 2010 Jul 1;26(13):1608-15.
[53] Resch A, Rosenstein R, Nerz C, Gotz F. Differential gene expression profiling of *Staphylococcus aureus* cultivated under biofilm and planktonic conditions. Appl Environ Microbiol 2005 May;71(5):2663-76.
[54] Cline MS, Smoot M, Cerami E, Kuchinsky A, Landys N, Workman C, et al. Integration of biological networks and gene expression data using Cytoscape. Nat Protoc 2007;2(10):2366-82.
[55] Wijtzes T, de Wit JC, In H, Van't R, Zwietering MH. Modelling Bacterial Growth of *Lactobacillus curvatus* as a Function of Acidity and Temperature. Appl Environ Microbiol 1995 Jul;61(7):2533-9.
[56] Stewart PS, Franklin MJ. Physiological heterogeneity in biofilms. Nat Rev Microbiol 2008 Mar;6(3):199-210.
[57] Westermann AJ, Gorski SA, Vogel J. Dual RNA-seq of pathogen and host. Nat Rev Microbiol 2012 Sep;10(9):618-30.
[58] Fang Z, Cui X. Design and validation issues in RNA-seq experiments. Brief Bioinform 2011 May;12(3):280-7.
[59] Tarazona S, Garcia-Alcalde F, Dopazo J, Ferrer A, Conesa A. Differential expression in RNA-seq: a matter of depth. Genome Res 2011 Dec;21(12):2213-23.
[60] Bullard JH, Purdom E, Hansen KD, Dudoit S. Evaluation of statistical methods for normalization and differential expression in mRNA-Seq experiments. BMC Bioinformatics 2010;11:94.
[61] Young MD, Wakefield MJ, Smyth GK, Oshlack A. Gene ontology analysis for RNA-seq: accounting for selection bias. Genome Biol 2010;11(2):R14.
[62] Blumenthal HJ, Huettner CF, Montiel FA. Comparative aspects of glucose catabolism in *Staphylococcus aureus* and *S. epidermidis*. Ann N Y Acad Sci 1974 Jul 31;236(0):105-14.
[63] Allison KR, Brynildsen MP, Collins JJ. Metabolite-enabled eradication of bacterial persisters by aminoglycosides. Nature 2011 May 12;473(7346):216-20.
[64] Shu M, Wong L, Miller JH, Sissons CH. Development of multi-species consortia biofilms of oral bacteria as an enamel and root caries model system. Arch Oral Biol 2000 Jan;45(1):27-40.
[65] Cotter PD, Hill C. Surviving the acid test: responses of gram-positive bacteria to low pH. Microbiol Mol Biol Rev 2003 Sep;67(3):429-53.
[66] Bhatt AN, Shukla N, Aliverti A, Zanetti G, Bhakuni V. Modulation of cooperativity in *Mycobacterium tuberculosis* NADPH-ferredoxin reductase: cation-and pH-induced alterations in native conformation and destabilization of the $NADP^+$-binding domain. Protein Sci 2005 Apr;14(4):980-92.

[67] Gill SR, Fouts DE, Archer GL, Mongodin EF, Deboy RT, Ravel J, et al. Insights on evolution of virulence and resistance from the complete genome analysis of an early methicillin-resistant *Staphylococcus aureus* strain and a biofilm-producing methicillin-resistant *Staphylococcus epidermidis* strain. J Bacteriol 2005 Apr;187(7):2426-38.
[68] Oliver JD. The viable but nonculturable state in bacteria. J Microbiol 2005 Feb;43 Spec No:93-100.
[69] Bink A, Vandenbosch D, Coenye T, Nelis H, Cammue BP, Thevissen K. Superoxide dismutases are involved in *Candida albicans* biofilm persistence against miconazole. Antimicrob Agents Chemother 2011 Sep;55(9):4033-7.
[70] Kint CI, Verstraeten N, Fauvart M, Michiels J. New-found fundamentals of bacterial persistence. Trends Microbiol 2012 Dec;20(12):577-85.
[71] Fu Z, Donegan NP, Memmi G, Cheung AL. Characterization of $MazF_{Sa}$, an endoribonuclease from *Staphylococcus aureus*. J Bacteriol 2007 Dec;189(24):8871-9.
[72] Schuster CF, Park JH, Prax M, Herbig A, Nieselt K, Rosenstein R, et al. Characterization of a mazEF toxin-antitoxin homologue from Staphylococcus equorum. J Bacteriol 2013 Jan;195(1):115-25.
[73] Li GW, Xie XS. Central dogma at the single-molecule level in living cells. Nature 2011 Jul 21;475(7356):308-15.
[74] Butala M, Klose D, Hodnik V, Rems A, Podlesek Z, Klare JP, et al. Interconversion between bound and free conformations of LexA orchestrates the bacterial SOS response. Nucleic Acids Res 2011 Aug;39(15):6546-57.
[75] Pavlidis P, Noble WS. Matrix2png: a utility for visualizing matrix data. Bioinformatics 2003 Jan 22;19(2):295-6.

Supplementary data

Table S1: Uniquely expressed genes in *S. epidermidis* grown in 1% G or 1% G + Mg^{2+}, and their known functions

1% G		1% G + Mg^{2+}	
Gene	**Description**	**Gene**	**Description**
serp0544	ISSep1-like transposase	*arsA*	Arsenical pump-driving ATPase
serp2458	CRISPR-associated protein, TM1808 family	*serp1626*	Uncharacterized protein
thyA-2	Thymidylate synthase, provides the sole de novo source of dTMP for DNA biosynthesis	*rrsB*	16S ribosomal RNA
		serp2217	Cytosine/purines, uracil, thiamine, allantoin, permease family protein
serp1340	ISSep1-like transposase	*serp1627*	Uncharacterized protein
serp1462	Hypothetical protein	*serp2471*	Type I restriction-modification system S subunit, EcoA family
serp1466	Tn554-related, transposase A		
serp1541	Uncharacterized protein	*serp2456*	Uncharacterized protein
serp1593	Uncharacterized protein	*serp1639*	Site-specific recombinase, phage integrase family
serp1580	Uncharacterized protein	*serp2218*	ADP-ribosylglycohydrolase
serp0042	Uncharacterized protein	*serp2494*	Uncharacterized protein
serp2163	IS1272-like transposase	*serp1601*	Site-specific recombinase, phage integrase family
serp0462	Uncharacterized protein	*serp1506*	Uncharacterized protein
serp2225	Transcriptional regulator, ArsR family	*serp2459*	CRISPR-associated protein, TM1792 family
serp0456	Uncharacterized protein	*serp1646*	Uncharacterized protein
serp0391	Pseudogene, transposase	*serp1514*	Uncharacterized protein
serp1096	Uncharacterized protein	*serp1631*	Uncharacterized protein
serp1527	Uncharacterized protein	*serp1533*	Uncharacterized protein
serp1479	Uncharacterized protein	*serp1536*	Uncharacterized protein
serp2468	Uncharacterized protein	*serp1635*	Uncharacterized protein

serp1905	Uncharacterized protein
mazE	Antitoxin component of a toxin-antitoxin module. Forms a complex with MazF which inhibits its endoribonuclease activity
serp1162	Uncharacterized protein
serp1628	Uncharacterized protein
serp0019	Uncharacterized protein
serp1447	Uncharacterized protein
serp1890	Uncharacterized protein
serp1629	Uncharacterized protein
serp1922	Uncharacterized protein
serp1841	Uncharacterized protein
rpmG-2	50S ribosomal protein L33
serp1418	UPF0435 protein (uncharacterized protein family)
serp2104	Uncharacterized protein

Table S2: Primers used in qPCR amplification

Target gene	Primer sequence (5' to 3')	Melting temperature (ºC)	Amplicon size (bp)
acnA	FW catattggcctaccggagaa RV tcacgagaagatcccattcc	60	118
pgi	FW tactacgacagaaccagcag RV catcaggtacaacaaacgtc	59	170
gapA-2	FW agcacctgttgacgttgga RV accagttgcaaaagtcctcaat	60	171
16S rRNA	FW gggctacacacgtgctacaa RV gtacaagacccgggaacgta	60	176
ureA	FW gttgtagctgctgaggttgc RV agctacgccatccatgacat	59	183
ctsR	FW tacaacgcgctcatattgct RV cgccaccacgtttactttct	60	117
rplE	FW acgtgacttccaaggtgtttc RV tcctcgtcagtgttagcagtt	60	162

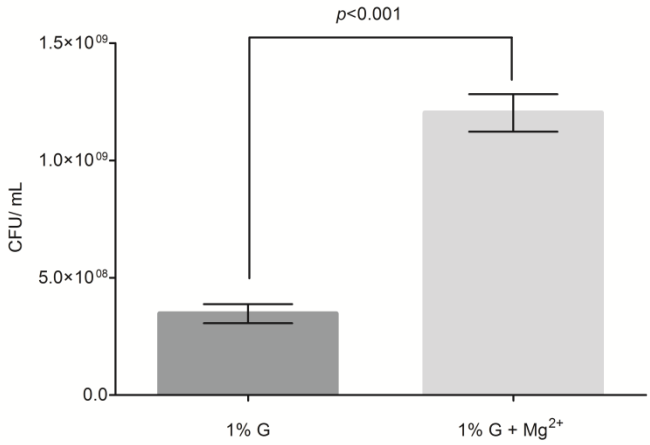

Fig. S1. Number of cultivable cells in *S. epidermidis* biofilm grown in 1% glucose and biofilms grown in 1% G plus 20mM of Mg^{2+}. The bars represent the mean and the error bars the standard error of the mean. Statistical significance was analyzed using unpaired t-test (with GraphPad Prism version 6).

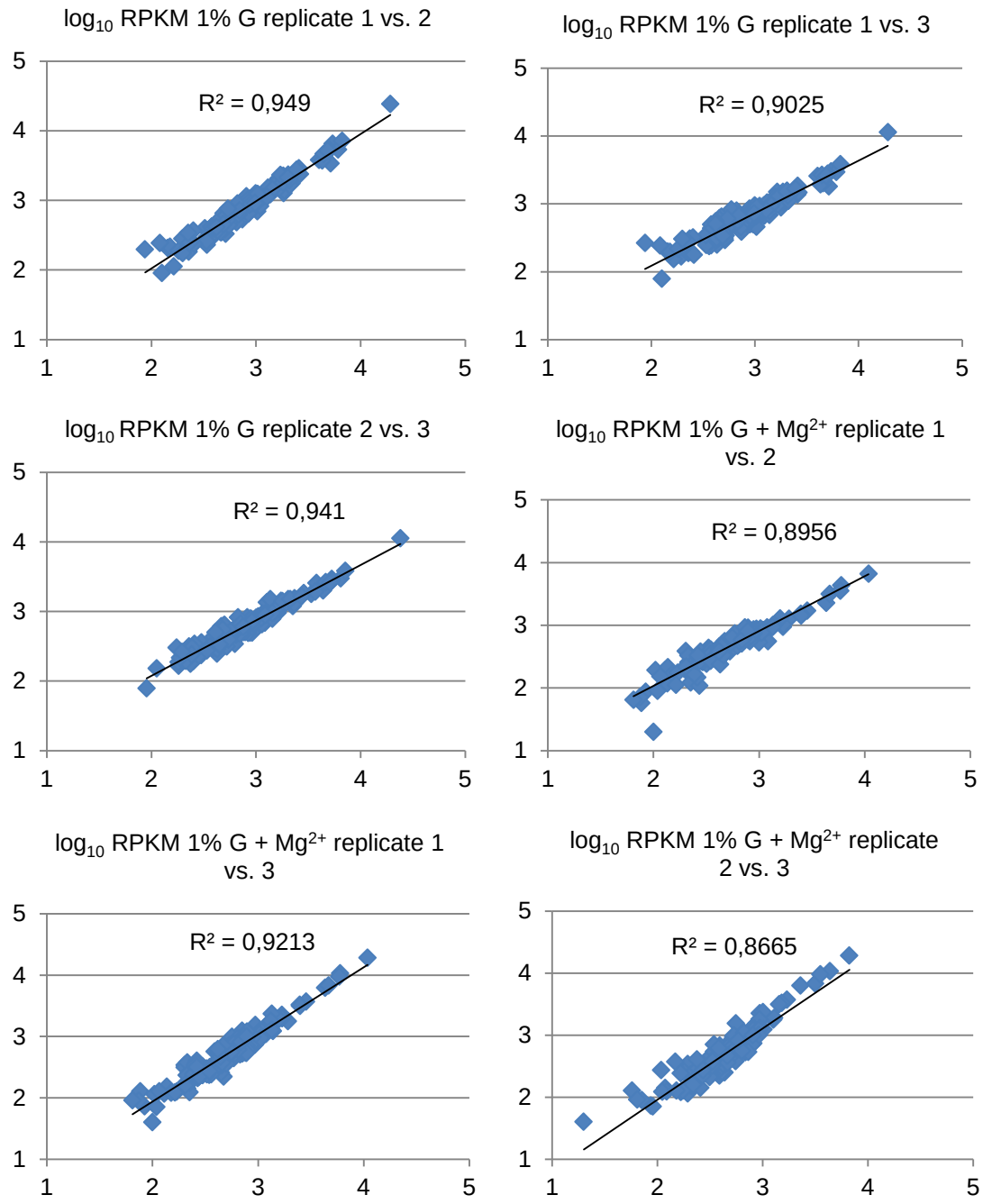

Fig. S2. Variation of $\log_{10}$ RPKM among the differentially expressed genes in biological triplicates

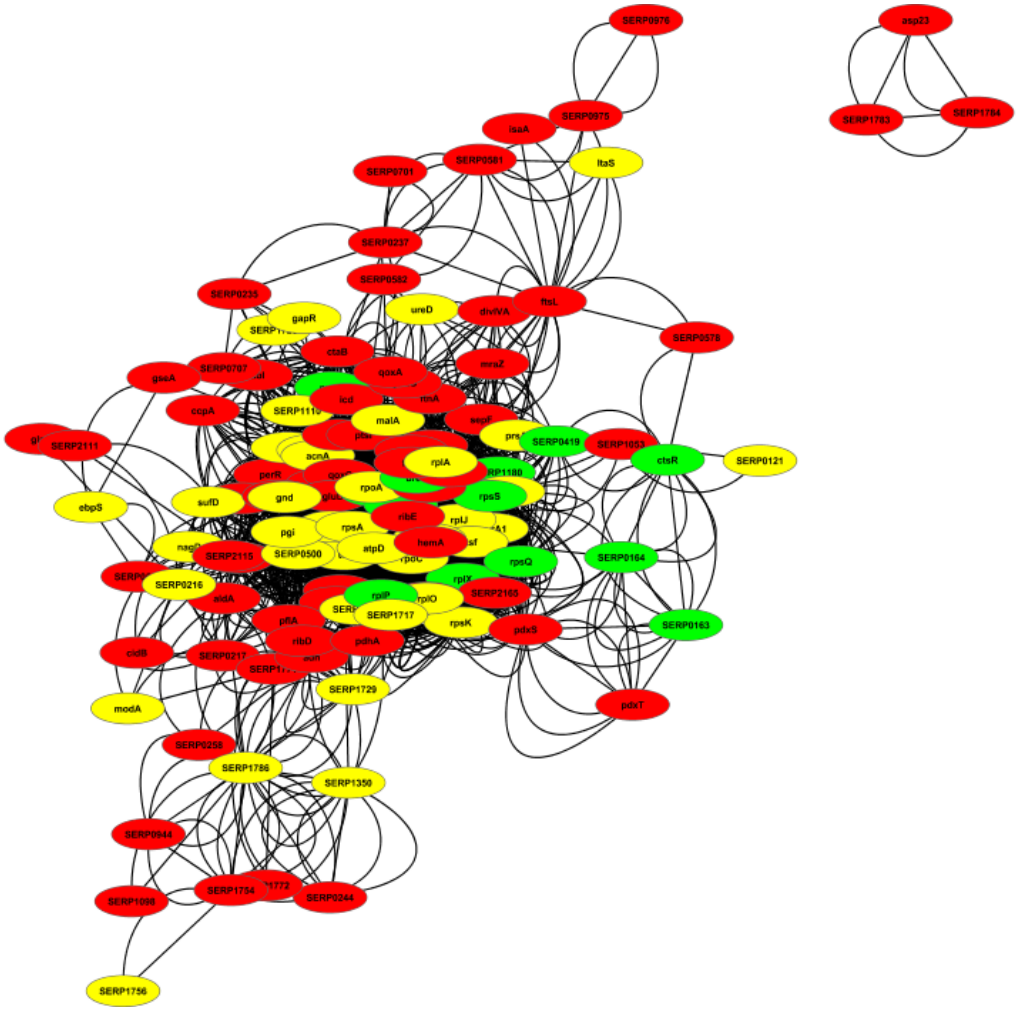

Fig. S3. Gene interaction network generated in Cytoscape with differently expressed genes, showing down-regulated transcripts (fold-change ≤ -1.50) in red and up-regulated transcripts (fold-change ≥1.50) in green. Yellow circles correspond to transcripts differentially expressed with a fold-change between -1.50 and 1.50